IEEE Open Journal of the
Industrial Electronics Society

Received 23 June 2020; revised 24 July 2020; accepted 25 July 2020. Date of publication 30 July 2020;
date of current version 14 August 2020. The review of this paper was arranged by Associate Editor W. Xu.

Digital Object Identifier 10.1109/OJIES.2020.3013249

Remote Control Method With Force Assist Based on Time to Collision for Mobile Robot

RYO MASAKI (Member, IEEE), AND NAOKI MOTOI (Member, IEEE)

(Invited Paper)

Kobe University, Kobe 658-0022, Japan

CORRESPONDING AUTHOR: NAOKI MOTOI (e-mail: motoi@maritime.kobe-u.ac.jp).

This work was supported by JSPS KAKENHI under Grant 19K04454, and the JGC-S Scholarship Foundation.

ABSTRACT This paper proposes a remote control method with the force assist to improve the operability of a mobile robot. The force feedback is generated on the basis of the time to collision (TTC) and translational velocity. The TTC is calculated from the predicted trajectory and environmental information, and is used as an indicator of the possibility of collision. If the possibility of collision is low, the force assist is not implemented. Therefore, the operator can control the mobile robot with a low manipulation force. On the contrary, if the collision possibility is high, the force assist is implemented. This force assist is classified on the bases of two cases according to the translational velocity. In the case of the low translational velocity, collision avoidance can be achieved via modification of the angular velocity alone. As a result, the proposed method generates a force assist for the angular velocity alone. On the contrary, if the translational velocity is high, it is necessary to modify both the translational and angular velocities to avoid collision. In this case, a force assist is generated for both velocities. Finally, the operability improvement resulting from the proposed method is confirmed experimentally.

INDEX TERMS Force control, mobile robot, motion control, robotics, remote control.

I. INTRODUCTION

The progress in robotic technology has been increasing at an accelerated pace. Robots are being increasingly used in hazardous and dangerous areas to replace human laborers. In particular, wheeled and caterpillar mobile robots have been developed and researched [1], [2]. In terms of the control method for mobile robots, remote control robots are more flexible than autonomous control robots because of their ability to perform several additional tasks on the basis of the operator's judgment.

Numerous types of remote control robots have been researched [3]. Zhang *et al.* proposed a remote control platform for an underwater manipulator mounted on a submersible vehicle, which operated on the basis of the visual information [4]. Sanders *et al.* reported a system wherein a mobile robot could change direction if there are environmental points ahead or it is helpful through using ultra sonic sensors [5]. These remote control robots allowed us to perform several tasks according to the operator's judgments. However, as the operator had to recognize the environment from visual information, several levels of trainings were necessary for skilled operation.

One approach to overcome the aforementioned problem of operability is by using remote control methods with force feedback [6], [7]. Shahzad *et al.* researched bilateral control of a mobile robot, on the basis of the distance and friction between the environment and robot [8]. Pecka *et al.* proposed a robot equipped with an arm containing a sensor [9]. Using the arm, the operator could feel the environment through tactile sensations. Bechet *et al.* proposed a novel electrohydraulic haptic transmission system to improve a surgery robot with a haptic system [10]. Motoi *et al.* developed the remote control method further, using the force feedback generated by collision prediction [11].

However, the conventional methods with force assist could not provide operability improvement. Conservative force assist techniques were used by the conventional methods to avoid collisions. Even when the possibility of collision was

low, the force assist generated was the same as that generated for a high possibility of collision. If such excessive force assist was used when the possibility of collision was low, the operability improvement could not be guaranteed.

The potential field method is one of the useful methods for generating a force assist for the remote control robots. Typically, the potential field is generated on the basis of the kinematic relationship between a robot and its obstacles. This potential value is treated as the possibility of collision. In order to generate force assist according to the possibility of collision, the force assist is generated on the basis of the gradient of the potential field. Therefore, a force assist suitable for the safe operation is generated. However, such a force assist may be excessive. The excessive force assist improves safety but deteriorates operability.

In this study, operability improvement is achieved via generation of a force assist that is as small as that required for avoiding collisions. In order to minimize the force assist, the proposed method divides the force assist on the basis of two cases according to the time to collision (TTC) and the translational velocity. In *Case 1*, the force assist is applied only to the angular velocity, since the mobile robot can avoid collision by modifying the angular velocity alone. In *Case 2*, modification of both the translational and angular velocities is necessary for collision avoidance. In such a case, force feedback is provided for both velocities. The proposed method generates the minimum force assist necessity to avoid collision. Through the proposed method, the operability can be improved while ensuring safety.

The authors had previously proposed the use of a data compression method to reduce the communication delay in the remote control method with force assist, which was confirmed [12]. However, the remote control method applied was the same as the one used in the conventional method. Therefore, the operability improvement was not validated in [12]. This paper proposes a remote control method with force assist to improve the operability. The force feedback is the minimum required value for collision avoidance while ensuring safety. The operability improvement is demonstrated by the experimental results presented in this paper.

This study presents two primary contributions, as mentioned below.

1) This paper proposes using a force assist that is as small as required for collision avoidance. The proposed method generates only that amount of force assist that is necessary to improve the operability. The proposed force feedback is generated on the basis of the TTC and the translational velocity. Using the force assist, the operator modifies the manipulation of the control device to avoid collision of the mobile robot. The force assist is not generated if the possibility of collision is low.

2) The operability improvement is confirmed from the experimental results. Ten subjects participated in the experiments to evaluate the operability. The experimental results demonstrated that the proposed method improves the operability when compared to the conventional method.

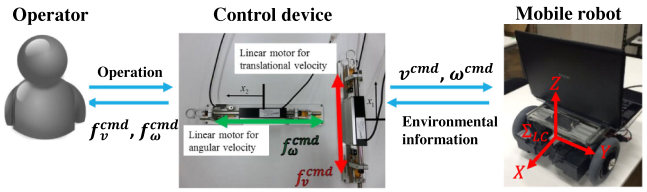

FIGURE 1. System configuration.

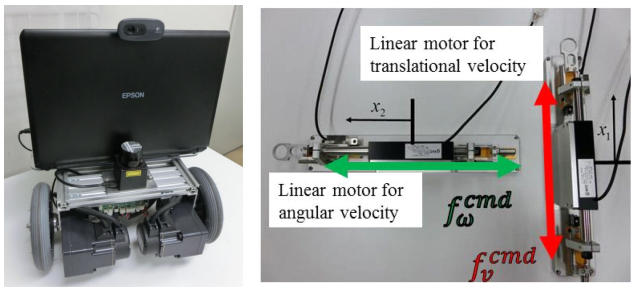

(a) Mobile robot (b) Control device

FIGURE 2. Mobile robot and control device.

The remainder of this paper is organized as follows. Section II presents an overview of the remote control system. Section III describes the conventional method of force assist [13]. Section IV proposes the force assist for the remote control of the mobile robot. Section V presents the experimental results for the comparison between the proposed and conventional methods. The conclusions are presented in Section VI.

II. REMOTE CONTROL SYSTEM

This section shows the remote control system with the force assist [12], [14].

A. SYSTEM CONFIGURATION

This subsection explains the system configuration shown in Fig. 1. This remote control system consists of the mobile robot and control device. The laser range finder (LRF) and visual sensor are attached to the mobile robot. Environmental information is measured by the LRF. In contrast, the velocity commands are generated during operation.

Fig. 2(a) shows the mobile robot [15]. As shown in Fig. 2(b), two linear motors are utilized as the control device for the translational and angular velocities. The operator manipulates the control device while watching the display. The force assist is generated simultaneously.

B. MODELING OF MOBILE ROBOT

This paper defines the global coordinate system Σ_{GL} and local coordinate system Σ_{LC}. The origin in Σ_{GL} is set to the initial position of the mobile robot. The direction of robot movement is along the X-axis, with the Y-axis on vertical left. The center of the mobile robot is set to the origin in Σ_{LC}.

The velocity relationship between Σ_{GL} and Σ_{LC} is calculated.

$$^{GL}\dot{x} = v\cos{}^{GL}\theta \tag{1}$$

$$^{GL}\dot{y} = v\sin{}^{GL}\theta \tag{2}$$

$$^{GL}\dot{\theta} = \omega \tag{3}$$

where ^{GL}x, ^{GL}y and $^{GL}\theta$ are the mobile robot position and orientation, respectively. $^{GL}\bigcirc$ represents the corresponding values in Σ_{GL}. The superscript is not utilized for the values in Σ_{LC}. v and ω indicate the translational and angular velocities, respectively.

The mobile robot position and orientation in Σ_{GL} are shown in the following equations.

$$^{GL}x = \int_0^t v\cdot\cos{}^{GL}\theta\, dt \tag{4}$$

$$^{GL}y = \int_0^t v\cdot\sin{}^{GL}\theta\, dt \tag{5}$$

$$^{GL}\theta = \int_0^t \omega\, dt \tag{6}$$

where t represents the moving time.

C. VELOCITY COMMAND GENERATOR

The translational velocity command v^{cmd} and angular velocity command ω^{cmd} are calculated from the movement of the control device.

$$v^{\mathrm{cmd}} = V^{\max}\cdot x_1^{res}/L^{\max} \tag{7}$$

$$\omega^{\mathrm{cmd}} = \Omega^{\max}\cdot x_2^{res}/L^{\max} \tag{8}$$

where $V^{\max}$ and $\Omega^{\max}$ indicate the maximum values of the translational and angular velocities, respectively. x_1 and x_2 represent the movement values of the control device. The superscripts $\bigcirc^{res}$ and $\bigcirc^{\mathrm{cmd}}$ indicate the response and command values, respectively. $L^{\max}$ is maximum displacement of the control device. These velocity commands are sent to the mobile robot.

D. FORCE CONTROLLER

The mobile robot is controlled by the operator through using the control device. Additionally, environmental information is sent to the operator through the tactile sensations from the control device. The disturbance observer (DOB) is used for the acceleration control in each linear motor [16]. The force controllers are implemented for the force feedback.

$$\ddot{x}_1^{\mathrm{ref}} = K_f(f_v^{\mathrm{cmd}} - \hat{f}_v^{ext}) \tag{9}$$

$$\ddot{x}_2^{\mathrm{ref}} = K_f(f_w^{\mathrm{cmd}} - \hat{f}_w^{ext}) \tag{10}$$

where $\ddot{x}_1^{\mathrm{ref}}$ and $\ddot{x}_2^{\mathrm{ref}}$ express the acceleration references. f_v^{cmd} and f_ω^{cmd} represent the force commands for the translational and angular velocities, respectively. $\hat{f}_v^{ext}$ and $\hat{f}_\omega^{ext}$ represent the estimation values of the external force by the reaction force observer (RFOB) [17]. K_f represents the force gain. Using (9) and (10), it is possible to generate the required force assist.

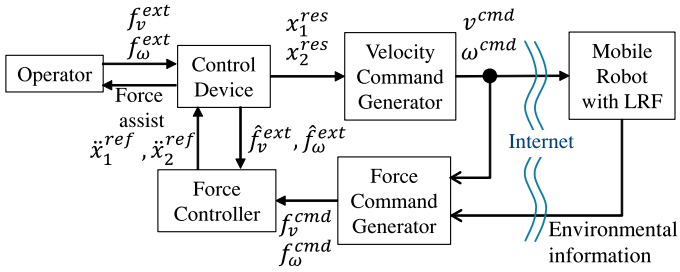

FIGURE 3. Block diagram of entire remote control system.

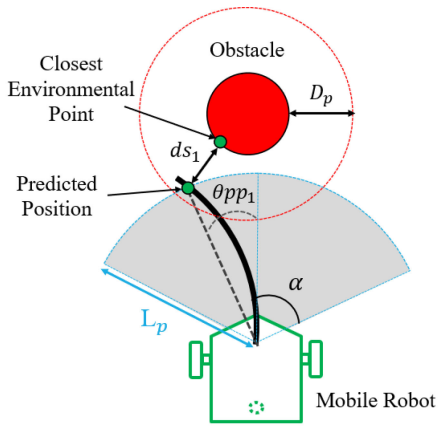

FIGURE 4. Configuration of force feedback for conventional method ($i = 1$).

E. ENTIRE REMOTE CONTROL SYSTEM

Fig. 3 shows the block diagram of the entire control system. The operator manipulates the control device for the remote control. v^{cmd} and ω^{cmd} are calculated in the velocity command generator, according to the manipulations of the operator. These velocity commands are applied to the mobile robot. During the movement of the mobile robot, environmental information is measured by the LRF. In the force command generator, the force commands for the force assist are calculated from environmental information, and velocity commands. The force feedback is generated in the control device, and the force assist to the operator is produced.

III. CONVENTIONAL METHOD

This section explains the force assist to avoid collision as the conventional method [13]. The force feedback is generated on the basis of a predicted position of the mobile robot after a translation of L_p in the current input direction of the control device. The force feedback is reflected along the translational direction of the control device only.

Fig. 4 shows the configuration of the force feedback for the conventional method. When the predicted position of the mobile robot is within the detection distance D_p of the obstacle,

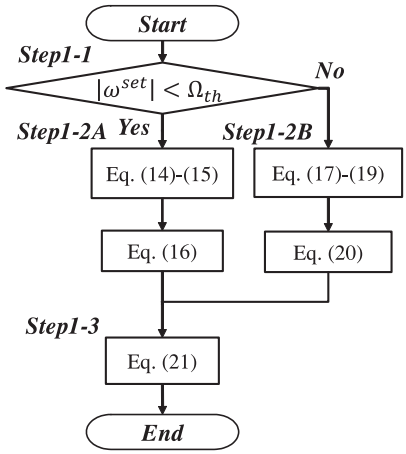

FIGURE 5. Flowchart of calculating time to collision.

a force feedback is generated on the basis of the distance L_p from the current position of the mobile robot. In the conventional method, the number of obstacles is defined as n. For each obstacle i ($i = 1, 2, \ldots, n$), this force feedback with gain K_p is proportional to the penetration depth ($D_p - ds_i$). ds_i is the distance between the predicted position of the mobile robot and the closest environmental point. In addition, the force feedback is only reflected to the control device when the mobile robot tends to move toward obstacles. When the obstacle is located within a detection angle α of the mobile robot, this force assist is achieved only by activating the force feedback. The force command f_i^{cmd} as the force feedback is expressed as follows.

$$f_i^{\mathrm{cmd}} = \begin{cases} K_p \cdot L_p \cdot (D_p - ds_i) & \text{if } ds_i \leq D_p \text{ and } |\theta pp_i| \leq \alpha \\ 0.0 & \text{otherwise} \end{cases} \tag{11}$$

where θpp_i is the angle between the translational direction of the mobile robot and the predicted direction. The force command f_v^{cmd} is the sum of the force commands f_i^{cmd} for all obstacles, and f_ω^{cmd} is set to 0 as follows.

$$f_v^{\mathrm{cmd}} = \sum_{i=1}^{n} f_i^{\mathrm{cmd}} \tag{12}$$

$$f_\omega^{\mathrm{cmd}} = 0.0 \tag{13}$$

IV. PROPOSED METHOD

This section presents the proposed force assist which is as small as the minimum amount required to achieve collision avoidance. The force feedback is calculated on the basis of the time to collision (TTC). Fig. 5 shows the flowchart for calculating the TTC. The TTC is calculated from the predicted trajectory and environmental information.

Step 1-1: The superscript $\bigcirc^{\mathrm{set}}$ indicates the values used in the calculation of the TTC. The robot motion is classified using the relationship of $|\omega^{\mathrm{set}}|$ and Ω_{th}. Ω_{th} indicates the threshold value of the angular velocity. Ω_{th} should be set to a value close to 0.

Step 1-2 A: In the case of $|\omega^{\mathrm{set}}| < \Omega_{th}$, the robot moves in a straight line. During straight motion, the area with the high collision probability is expressed as follows.

$$y_l^s > -D \tag{14}$$

$$y_l^s < D \tag{15}$$

where y_l^s ($l = 1, 2, \ldots, M$) is the environmental position along the Y-axis. M is the number of the measurement points of the LRF. D represents the half width of the mobile robot. The closest environment for the mobile robot in (14) and (15) is extracted as $(x_{\min}^s, y_{\min}^s)$. The distance to this environment is expressed.

$$l^s = x_{\min}^s \tag{16}$$

where l^s is the distance from the closest environment that may collide.

Step 1-2B: In the case of $|\omega^{\mathrm{set}}| \geq \Omega_{th}$, the robot moves along a circular trajectory. The turning radius r^{set} is expressed in terms of the translational velocity v^{set} and ω^{set}.

$$r^{\mathrm{set}} = \frac{v^{\mathrm{set}}}{\omega^{\mathrm{set}}} \tag{17}$$

During circular motion, the area with a high collision probability is expressed as follows.

$$(x_l^s - 0)^2 + (y_l^s - r^{\mathrm{set}})^2 > (|r^{\mathrm{set}}| - D)^2 \tag{18}$$

$$(x_l^s - 0)^2 + (y_l^s - r^{\mathrm{set}})^2 < (|r^{\mathrm{set}}| + D)^2 \tag{19}$$

where x_l^s ($l = 1, 2, \ldots, M$) is the environmental position along the X-axis. The closest environmental position from the mobile robot in (18) and (19) has the highest possibility of collision. The angle of the closest environmental point from the center of the turning for the mobile robot is defined as $\theta_{\min}^s$. The distance to this environment is expressed.

$$l^s = r^{\mathrm{set}} \theta_{\min}^s \tag{20}$$

Step 1-3: The TTC t_{ttc} is calculated as follows.

$$t_{ttc} = \frac{l^s}{v^{\mathrm{set}}} \tag{21}$$

where the superscript $\bigcirc_{ttc}$ indicates the value of the TTC.

Fig. 6 shows the flowchart for the proposed method. This flowchart consists of five steps.

Step 0: The translational and angular velocity responses are assigned to v^{set} and ω^{set} as follows.

$$v^{\mathrm{set}} = v^{res} \tag{22}$$

$$\omega^{\mathrm{set}} = \omega^{res} \tag{23}$$

By using (22) and (23), the turning radius response r^{set} is calculated on the basis of (17).

Step 1: By using the calculation method of the TTC as shown in Fig. 5, the TTC of v^{set} and ω^{set} is calculated as t_{ttc}^{res}.

Step 2: In the case of $t_{ttc}^{res} > T_{th}$, the mobile robot is considered to have low collision possibility. T_{th} is the time threshold for safe operation. In this case, it is not necessary to modify

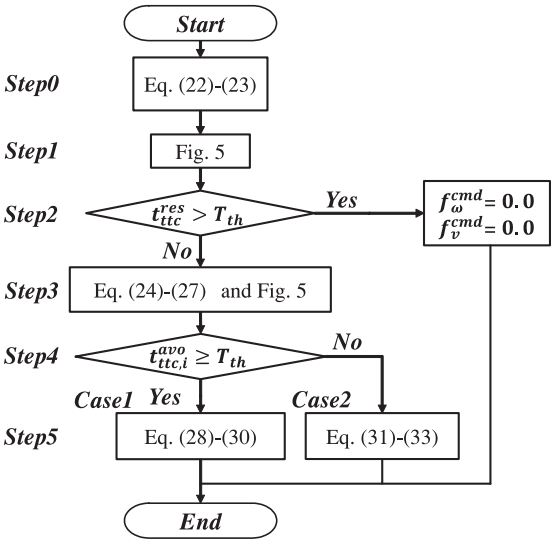

FIGURE 6. Flowchart for proposed method.

the velocity commands. Therefore, there is no force feedback ($f_v^{\text{cmd}} = f_\omega^{\text{cmd}} = 0.0$) and the control moves to *END* from *Step 2*.

In contrast, in the case of $t_{ttc}^{res} \leq T_{th}$, the mobile robot is considered to have high collision possibility. Furthermore, the control moves from *Step 2* goes to *Step 3* to generate the force commands.

By setting T_{th} to a high value, safe remote control is achieved. However, the frequency force commands are generated according to the environment conditions, and could not provide operability improvement.

Step 3: The superscript $\bigcirc^{avo}$ indicates the prediction value required to avoid the obstacle. The all predicted turning radius r_i^{avo} $(i = 0, 1, 2, \ldots, N-1)$ and the TTC $t_{ttc,i}^{avo}$ $(i = 0, 1, 2, \ldots, N-1)$ are calculated. $t_{ttc,i}^{avo}$ is the TTC of each predicted trajectory. r_i^{avo} is derived from the angle θ_i as shown in Fig. 7. θ_i is calculated as follows.

$$\theta_i = \frac{\pi}{N-1} \cdot i - \frac{\pi}{2} \tag{24}$$

where N and i indicate the number of trajectories and coefficient, respectively. The angular velocity of each predicted trajectory is defined as ω_i^{avo} $(i = 0, 1, 2, \ldots, N-1)$. ω_i^{avo} is calculated using r_i^{avo}. r_i^{avo} of each θ_i is calculated as follows.

$$r_i^{avo} = \frac{R_{th}}{2\sin(\theta_i)} \tag{25}$$

where R_{th} is the turning radius of the operating range as shown in Fig. 7(a). By setting R_{th} to a high value, the measurement area is increased. However, to maintain high spatial resolution for obstacle measurement, N should be increased according to R_{th}, which increases the calculation cost. From this viewpoint, it is necessary to decide R_{th} considering the calculation cost and safety according to the moving environment. By using

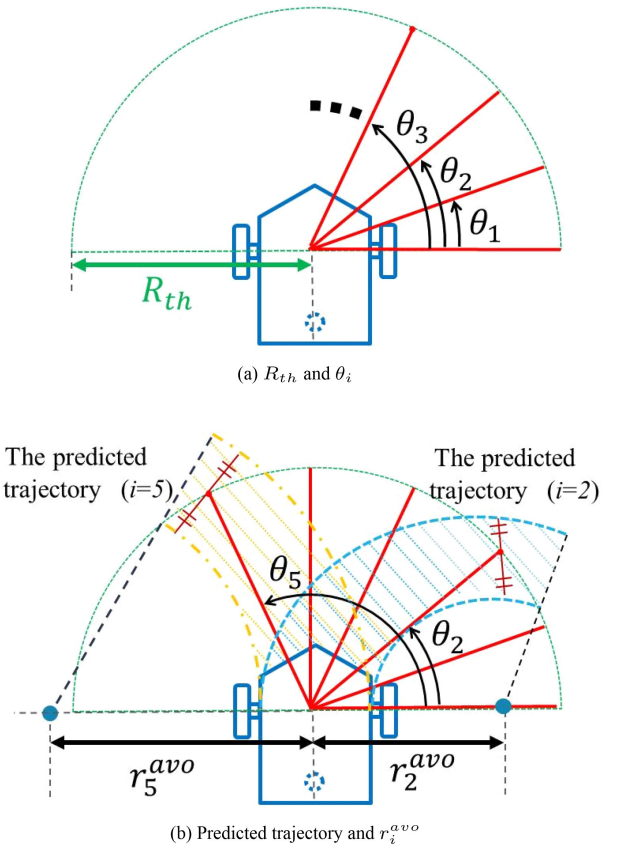

FIGURE 7. Relationship with angle θ_i and predicted trajectory.

(25), ω_i^{avo} of each θ_i is calculated.

$$\omega_i^{avo} = \frac{v^{res}}{r_i^{avo}} \tag{26}$$

v_{set} is kept as (22), and ω^{set} is updated as (27).

$$\omega^{\text{set}} = \omega_i^{avo} \tag{27}$$

On the basis of Fig. 5, $t_{ttc,i}^{avo}$ for each predicted trajectory is calculated from (22) and (27). Fig. 7(b) shows the predicted trajectories and r_i^{avo} at $i = 2$ and $i = 5$. The shaded area in the predicted trajectories of Fig. 7(b) indicates a high collision probability.

Step 4: All TTC $t_{ttc,i}^{avo}$ are compared with T_{th}. In the case of $\exists j \in A$ $(A = \{0, 1, 2, \ldots, N-1\})$, $t_{ttc,j}^{avo} \geq T_{th}$, the mobile robot can avoid collision by modifying only the angular velocity. The control moves from *Step 4* to *Step 5* as in *Case 1* to calculate the force command for the angular velocity.

In contrast, if $t_{ttc,i}^{avo} < T_{th}$, it is necessary for the mobile robot to modify the translational and angular velocities for collision avoidance. The control moves from *Step 4* to *Step 5* as in *Case 2* to calculate the force commands for both the translational and angular velocities.

Step 5: In *Case 1*, r_i^{avo} is decided to one of each predicted turning radius as r_p^{avo} at the moment. p is one of j which meets $t_{ttc,p}^{avo} \geq T_{th}$. The force command for the translational velocity

TABLE 1. Specification of Mobile Robot

Parameters	Description	Values
V^{max}	Maximum translational velocity	0.45m/s
V^{min}	Minimum translational velocity	0.0m/s
Ω^{max}	Maximum angular velocity	1.5rad/s
Ω^{min}	Minimum angular velocity	-1.5rad/s
$\dot{V}^{max}$	Maximum translational acceleration	1.0m/s^2
$\dot{\Omega}^{max}$	Maximum angular acceleration	2.0rad/s^2
D	Half width of mobile robot	0.19m

TABLE 2. Control Parameters

Parameters	Description	Values
Ω_{th}	Threshold value of angular velocity	0.01rad/s
K_v	Translational force feedback gain	3.0×10^6
K_ω	Angular force feedback gain	1.7
R_{th}	Operating range of collision-free	0.7m
N	Number of trajectories for searching	21
T_{th}	Time threshold for safe operation	10.0s
L_p	Distance threshold	0.7m
K_p	Force feedback gain	5.0
D_p	Detection distance of obstacles	0.7m
α	Detection angle	$\pi/2$rad
G_{LPF}	Cut-off gain of LPF	1.0

is set to 0 ($f_v^{\rm cmd} = 0.0$). The force commands in *Case 1* are calculated as follows.

$$f_v^{\rm cmd} = 0.0 \tag{28}$$

$$f_\omega^{\rm cmd} = K_\omega \cdot g_{LPF}(s) \cdot (r_p^{avo} - r^{res}) \tag{29}$$

$$g_{LPF}(s) = \frac{G_{LPF}}{s + G_{LPF}} \tag{30}$$

where K_ω is the angular force feedback gain. G_{LPF} is the cut-off gain of the low-pass filter (LPF), and s is the Laplace operator. This research implements the LPF for the smooth modification of the force commands.

In contrast, in *Case 2*, the mobile robot needs to modify the translational velocity for the recovery of the TTC. The largest TTC is extracted from $t_{ttc,i}^{avo}$, and i is set to q. In addition, v^{res} is modified to the translational velocity v^{avo}. The TTC and the translational velocity exhibit a linear relationship. By using this relationship, v^{avo} is calculated to meet the TTC that is equal to T_{th}.

$$v^{avo} = \frac{1}{T_{th}} \cdot t_{ttc,q}^{avo} \cdot v^{res} \tag{31}$$

The force commands in *Case 2* are generated.

$$f_v^{\rm cmd} = K_v \cdot g_{LPF}(s) \cdot (v^{avo} - v^{res}) \tag{32}$$

$$f_\omega^{\rm cmd} = K_\omega \cdot g_{LPF}(s) \cdot (r_q^{avo} - r^{res}) \tag{33}$$

where K_v is the translational force feedback gain.

V. EXPERIMENT

This section shows the experimental results to confirm the validity of the proposed method.

A. EXPERIMENTAL SETUP

The mobile robot specification and control parameters are expressed in Table 1 and Table 2, respectively. The experiments were conducted on 10 subjects who were not familiar with the operation of the robot. Therefore, T_{th} was set to a large value for ensuring safe operation. The operating range of collision-free R_{th} was decided considering the calculation cost and safety, according to the experimental course. The distance threshold L_p was synonymous with R_{th}. For fair comparison between the proposed method and conventional method, L_p was set to the same value as R_{th}. If the detection distance of obstacles D_p was smaller than L_p, the robot could collide with the obstacle. Therefore, in this research, D_p was set to almost the same value as that of L_p.

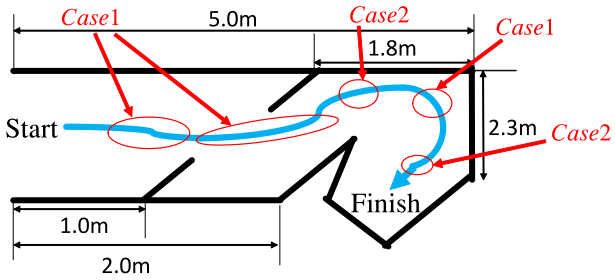

FIGURE 8. Experimental course (Cases are related to Fig. 10).

In order to experimentally prove the operability improvement, ten subjects (A-J) with an average age of 23.9 years and 1.97 year standard deviation, participated in the experiments. In these experiments, the subjects manipulated the mobile robot without being informed as to which methods were applied. Before the experiment was commenced, the subjects were allowed to practice to manipulating the mobile robot.

For the evaluation of operability, the subjects must perform straight/curved operations and obstacle avoidance operations. Therefore, the robot moved along a clockwise course with some obstacles shown in Fig. 8. In these experiments, it was necessary for subjects to perform operations to avoid collisions, from the start to finish. Each subject controlled the mobile robot using visual information displayed on a monitor. In addition, while each subject was in the process of manipulating the control device, force feedback was generated to the control device.

B. EXPERIMENTAL RESULTS

Figs. 9–10 show the experimental results of the conventional method and proposed method operated by Subject B. Fig. 11(a) and (b) show the experimental trajectory results and environmental information by the conventional and proposed methods. As shown in Fig. 11(a) and (b), the mobile robot moved from start point to finish.

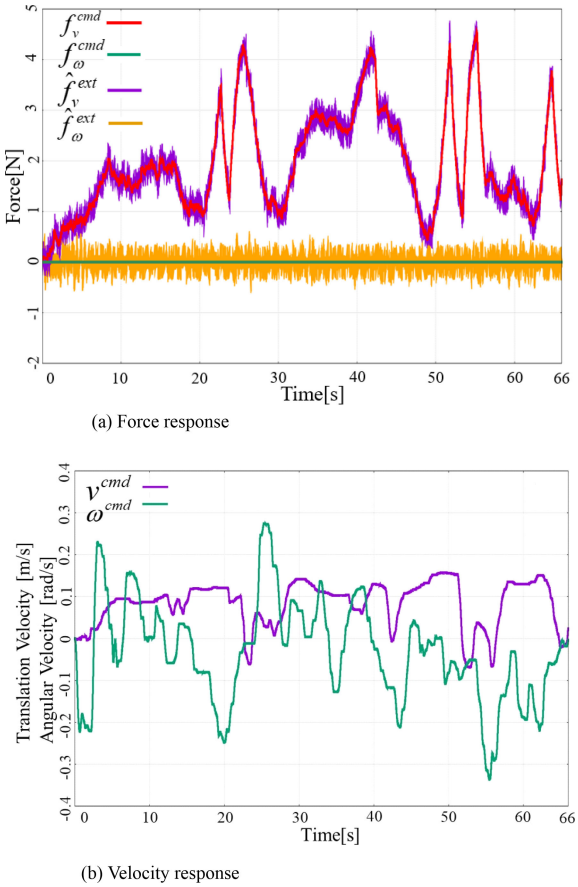

(a) Force response

(b) Velocity response

FIGURE 9. **Experimental results (conventional method).**

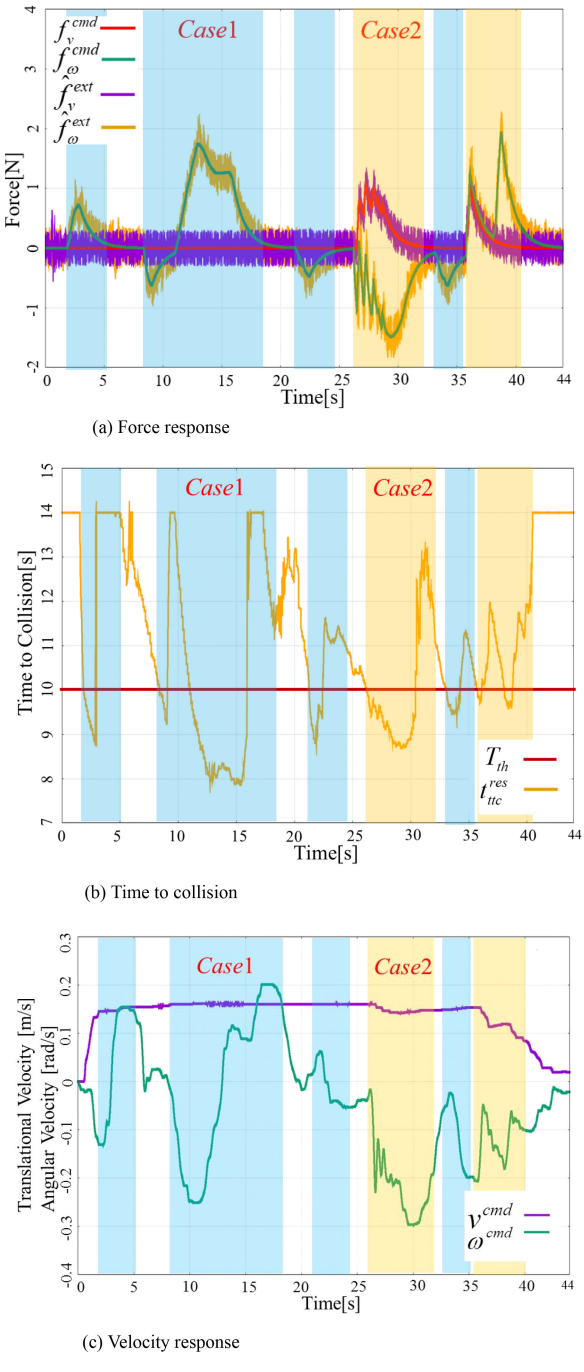

(a) Force response

(b) Time to collision

(c) Velocity response

FIGURE 10. **Experimental results (proposed method).**

Fig. 9(a) and (b) show the force responses and the velocity responses of the conventional method. As shown in Fig. 9(a), the force responses follow the force commands. This fact indicates that the force assist is achieved, and the subject has recognized environmental information as a tactile sensation. However, the force commands for the translational velocity are always generated during movement. In other words, this force assist is conservative. Therefore, the translational velocity command is fluctuated by the force assist as shown in Fig. 9(b).

Fig. 10(a), (b) and (c) illustrated the force responses, TTC, and velocity responses of the proposed method. In Fig. 10, the blue and orange shaded area represent the proposed force feedbacks in *Case 1* and *Case 2*. In Fig. 10(b), t_{ttc}^{res} which exceeds 14[s] was not indicated in this paper. This is because the possibility of collision is low over 14[s]. As shown in Fig. 10(a), the force responses follow the force commands, and the force assist is achieved. These force commands were generated according to the TTC and T_{th} as shown in Fig. 10(b). When the possibility of collision was low ($t_{ttc}^{res} > T_{th}$), the force commands were not generated ($f_v^{\mathrm{cmd}} = f_\omega^{\mathrm{cmd}} = 0.0$). Therefore, the operator could manipulate the remote control system with only a small force. When the possibility of collision was high ($t_{ttc}^{res} \leq T_{th}$), a force assist was generated.

As shown in *Case 1* of Fig. 10(a) and (c), only the force command for the angular velocity was generated, and the angular velocity was modified at the same time. In this case, the translational velocity remained almost the same value. On the other hand, in *Case 2*, both the force commands were calculated. Therefore, both the translational and angular velocities were modified. From these velocity results, it was clear that the force assist was the minimum value necessary for collision avoidance, as the velocity responses did not fluctuate, compared to that of the conventional method.

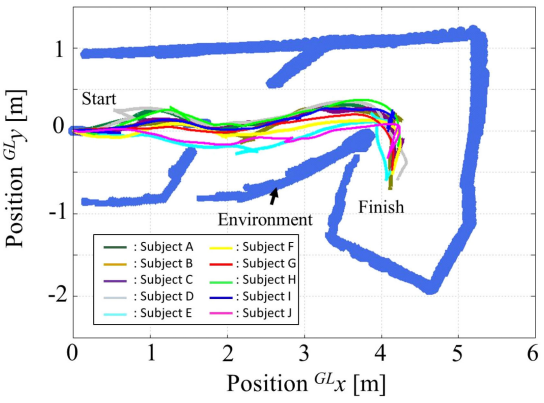

(a) Conventional method

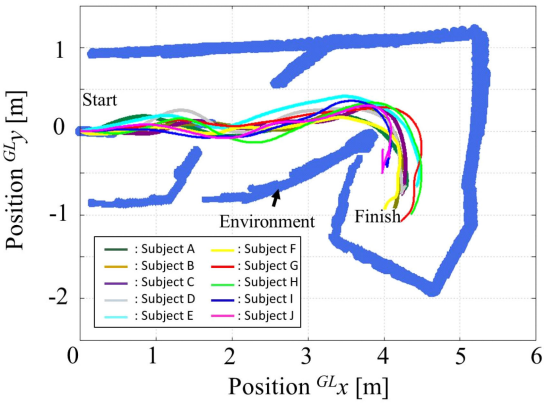

(b) Proposed method

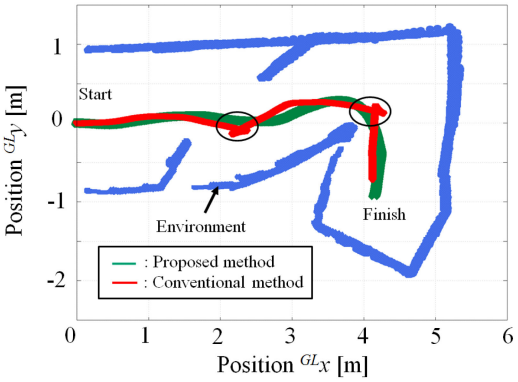

(c) Conventional and proposed methods by Subject B

FIGURE 11. **Experimental results of trajectories.**

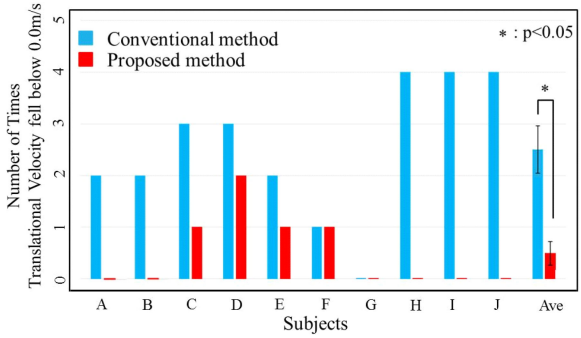

FIGURE 12. **Experimental results of number of times translational velocity fell below 0.0m/s.**

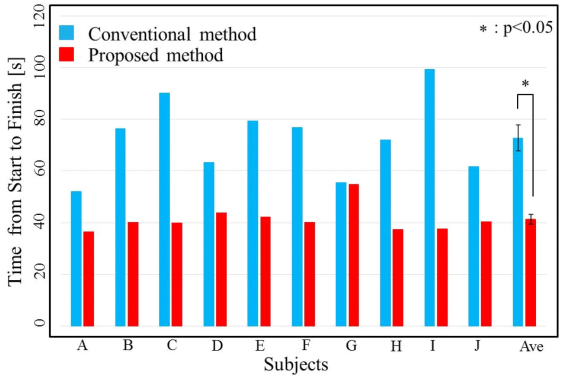

FIGURE 13. **Experimental results of time from start to finish.**

For comparison, Fig. 11(c) shows the results of the conventional and proposed methods operated by Subject B. In the conventional method, there were two points (black circles) which went back because of the obstacle. On the contrary, in the proposed method, there were no points that went back.

Fig. 12 shows the experimental results of the number of times the translational velocity fell below 0.0[m/s]. Fig. 13 shows the time from the start to finish. In Figs. 12–13, the error bars indicate the distribution of data and the horizontal bar indicates a significant difference over the factor environment or support, where $*$ denotes the significance of $p < 0.05$. $*$ means that there is a statistically significant difference.

As shown in Fig. 12, for 7 out of 10 subjects, the number of times the translational velocity fell below 0.0[m/s] was reduced when the proposed method was employed. For the remaining three subjects, this number of times was the same in both the conventional and proposed methods. Without subject G, for 9 out of 10 subjects, the time from the start point to the finish was improved by using the proposed method as shown in Fig. 13. For Subject G, the number of times the translational velocity fell below 0.0[m/s] was 0 for both the conventional and proposed methods. Focusing on Subject G in Fig. 13, the time for the proposed method and conventional method were almost equal. When the possibility of collision was low, the force assist did not work in both the proposed and conventional methods. This fact shows why the force assist did not work during the experiments for Subject G. Therefore, the experimental value of Subject G was treated as an outlier, in the comparisons between the proposed and conventional methods. From Figs. 12–13, the operability was found to have been improved by the proposed method, when compared to that of the conventional method. The validity of the proposed method was confirmed.

VI. CONCLUSION

This paper proposed a remote control method with a force assist on the basis of the TTC and translational velocity for mobile robots. The proposed force assist was the minimum value required for the collision avoidance. Therefore, the proposed method generated only the force assist that was required for operability improvement.

If the possibility of collision was low, a force feedback was not generated and the operator could operate the remote control system with a small force. In contrast, a force feedback was generated if the possibility of collision was high. The force command was generated according to the TTC and translational velocity. If the mobile robot could avoid collision by modifying only the angular velocity, the operator experienced a force assist along the angular direction. On the contrary, if it was necessary to modify the translational and angular velocities for collision avoidance, the force commands were generated for both velocities.

Ten subjects participated in the experiments to evaluate the operability. From the experimental results, it could be observed that the proposed method improved the operability when compared to that of the conventional method. Thus, the effectiveness of the operability improvement by the proposed method was confirmed experimentally.

The future work that can be conducted on the basis of this research is described as follows.

* The proposed method should be extended to moving obstacles.
* The design methods for several parameters should be developed.
* The evaluation function for operability should be developed for quantitative evaluation.

REFERENCES

[1] M. Minamoto, K. Kawashima and T. Kanno, "Effect of force feedback on a bulldozer-type robot," in *Proc. IEEE Int. Conf. Mechatronics Autom.*, 2016, pp. 2203–2208.

[2] W. Li, L. Ding, Z. Liu, W. Wang, H. Gao, and M. Tavakoli, "Kinematic bilateral teledriving of wheeled mobile robots coupled with slippage," *IEEE Trans. Ind. Electron.*, vol. 64, no. 3, pp. 2147–2157, Mar. 2017.

[3] S. Zhao, Z. Li, R. Cui, Y. Kang, F. Sun, and R. Song, "Brain-machine interfacing-based teleoperation of multiple coordinated mobile robots," *IEEE Trans. Ind. Electron.*, vol. 64, no. 6, pp. 5161–5170, Jun. 2017.

[4] J. Zhang *et al.*, "Development of a virtual platform for telepresence control of an underwater manipulator mounted on a submersible vehicle," *IEEE Trans. Ind. Electron.*, vol. 64, no. 2, pp. 1716–1727, Feb. 2017.

[5] D. A. Sanders, B. J. Sanders, A. Gegov, and D. Ndzi, "Using confidence factors to share control between a mobile robot tele-operator and ultrasonic sensors," in *Proc. Intell. Syst. Conf.*, 2017, pp. 1026–1033.

[6] T. Nozaki, S. Shimizu, T. Murakami, and R. Oboe, "Impedance field expression of bilateral control for reducing data traffic in haptic transmission," *IEEE Trans. Ind. Electron.*, vol. 66, no. 2, pp. 1142–1150, Feb. 2019.

[7] S. Sakaino, T. Furuya, and T. Tsuji, "Bilateral control between electric and hydraulic actuators using linearization of hydraulic actuators," *IEEE Trans. Ind. Electron.*, vol. 64, no. 6, pp. 4631–4641, Jun. 2017.

[8] A. Shahzad and H. Roth, "Bilateral telecontrol of automerlin mobile robot," in *Proc. Int. Conf. Open Source Syst. and Technol.*, vol. 14, pp. 1–6, 2015.

[9] M. Pecka, K. Zimmermann, M. Reinstein and T. Svoboda, "Controlling robot morphology from incomplete measurements," *IEEE Trans. Ind. Electron.*, vol. 64, pp. 1773–1150, Feb. 2017.

[10] F. Bechet, K. Ogawa, E. Sariyildiz and K. Ohnishi, "Electrohydraulic transmission system for minimally invasive robotics," *IEEE Trans. Ind. Electron.*, vol. 62, no. 12, pp. 7643–7654, Dec. 2015.

[11] H. Kimura and N. Motoi, "Virtual force generation method for remote control system in mobile robot," in *Proc. Annu. Conf. IEEE Ind. Electron. Soc.*, 2016, pp. 6193–6198.

[12] N. Motoi, R. Masaki, and M. Kobayashi, "Remote control method with force assist based on collision prediction calculated from each turning radius in mobile robot," in *Proc. IEEE Int. Conf. Mechatronics*, 2019, pp. 477–482.

[13] R. Kuiper, D. Heck, I. Kuling, and D. Abbink, "Evaluation of haptic and visual cues for repulsive or attractive guidance in nonholonomic steering tasks," *IEEE Trans. Human-Mach. Syst.*, vol. 46, no. 5, pp. 672–683, Oct. 2016.

[14] N. Motoi, H. Kimura, and M. Kobayashi, "Experimental operability evaluation of remote control with force feedback for mobile robot," in *Proc. IEEE Int. Conf. Ind. Technol.*, 2018, pp. 159–164.

[15] T-frog Project, [Online]. Available: https://t-frog.com/

[16] K. Ohnishi, M. Shibata, and T. Murakami, "Motion control for advanced mechatronics," *IEEE/ASME Trans. Mechatronics*, Vol. 1, no. 1, pp. 56–67, Mar. 1996.

[17] T. Murakami, F. Yu, and K. Ohnishi, "Torque sensorless control in multidegree-of-freedom manipulator," *IEEE Trans. Ind. Electron.*, vol. 40, no. 2, pp. 259–265, Apr. 1993.

RYO MASAKI (Member, IEEE) received the B.E. degree in marine engineering from Kobe University, Japan, in 2018. He is currently working towards the M.E. degree from the Graduate School of Maritime Sciences, Kobe University, Japan. He is also working towards the M.E. degree in advanced control and systems engineering, the University of Sheffield, United Kingdom. His current research interests include haptics and motion control.

NAOKI MOTOI (Member, IEEE) received the B.E. degree in system design engineering and the M.E. and Ph.D. degrees in integrated design engineering from Keio University, Japan, in 2005, 2007 and 2010, respectively. In 2007, he joined the Partner Robot Division, Toyota Motor Corporation, Japan. From 2011 to 2013, he was a Research Associate at Yokohama National University, Japan. Since 2014, he has been with Kobe University, Japan, where he is a currently Associate Professor. From 2019 to 2020, he also held the position of a Visiting Professor at Automation and Control Institute (ACIN), TU Wien, Austria. His current research interests include robotics, motion control, and haptic.